TMEM165, a Golgi transmembrane protein, is a novel marker for hepatocellular carcinoma and its depletion impairs invasion activity

JEE-SAN LEE[1*], MI-YEUN KIM[1,8*], EUN-RAN PARK[1], YAN NAN SHEN[1,10], JU-YEON JEON[1], EUNG-HO CHO[2], SUN-HOO PARK[3], CHUL JU HAN[4], DONG WOOK CHOI[5], JA JUNE JANG[6], KYUNG-SUK SUH[7], JUNGIL HONG[8], SANG BUM KIM[2] and KEE-HO LEE[1,9]

[1]Division of Radiation Cancer Research, Departments of [2]Surgery, [3]Pathology and [4]Internal Medicine, Division of Radiological and Clinical Research, Korea Institute of Radiological and Medical Sciences, Seoul 01812; [5]Department of Surgery, Samsung Medical Center, Sungkyunkwan University School of Medicine, Seoul 06351; [6]Departments of Pathology and [7]Surgery, Seoul National University School of Medicine, Seoul 08226; [8]Division of Applied Food System and [9]Department of Biotechnology, College of Natural Science, Seoul Women's University, Seoul 01797, Republic of Korea; [10]Key Laboratory of Radiobiology, School of Public health, Jilin University, Changchun, Jilin 130012, P.R. China

Abstract. Transmembrane protein 165 (TMEM165), a Golgi protein, functions in ion homeostasis and vesicular trafficking in the Golgi apparatus. While mutations in *TMEM165* are known to cause human 'congenital disorders of glycosylation', a recessive autosomal metabolic disease, the potential association of this protein with human cancer development has not been explored to date. In the present study, we revealed that *TMEM165* is overexpressed in HCC and its depletion weakens the invasive activity of cancer cells through suppression of matrix metalloproteinase-2 (MMP-2) expression. Levels of *TMEM165* mRNA and protein were clearly increased in HCC patient tissues and cell cultures. Quantitative real-time RT-PCR analysis of fresh HCC tissues (n=88) revealed association of *TMEM165* overexpression with more frequent macroscopic vascular invasion, microscopic serosal invasion and higher α-fetoprotein levels. Notably, depletion of *TMEM165* led to a marked decrease in the invasive activity of two different HCC cell types, Huh7 and SNU475, accompanied by downregulation of MMP-2. Our collective findings clearly indicated that TMEM165 contributed to the progression of HCC by promoting invasive activity, supporting its utility as a novel biomarker and therapeutic target for cancer.

Introduction

Hepatocellular carcinoma (HCC) is the most common form of primary liver cancer in adults and the third leading cause of cancer-related mortality worldwide (1). HCC occurs most frequently in patients with chronic liver disease and cirrhosis (2). The common risk factors of HCC include hepatitis B and C virus infection, heavy consumption of alcohol, exposure to aflatoxin B1 and non-alcoholic steatohepatitis (3). Despite significant advances in diagnosis and treatment, liver resection and transplantation are considered the only curative options at present (3). To date, no effective treatment strategies have been developed for patients with advanced HCC, including the approved therapeutic agent, sorafenib (4), owing to chemoresistance and excessive cytotoxicity resulting in dismal prognosis (5). Therefore, identification of early and effective diagnostic markers and therapeutic targets for this disease remains an urgent unmet medical need.

The discovery of genes involved in tumor progression has prompted research into various methods of therapeutic intervention. Based on advances in genome-wide technology in cancer research, we established a microarray dataset to identify the genes responsible for dismal prognosis in earlier studies (6-8). In the present study, transmembrane protein 165

(TMEM165), a Golgi protein (9), was shown to be associated with aggressive characteristics of HCC. TMEM165 is a highly conserved hydrophobic protein of 324 amino acids that contains 7 transmembrane-spanning domains according to topology predictions (10). Recent research has revealed that mutations in *TMEM165* were associated with a rare autosomal recessive disease designated 'congenital disorders of glycosylation' leading to defects in metabolic processes through impairment of galactosylation and sialylation of N-glycoproteins (10-14). The majority of congenital disorders of glycosylation are caused by defects in glycosylation machinery components, such as SLC35A1, B4GALT1 and MGAT2 (15-17). In contrast to the glycosylation-governing proteins, TMEM165 maintains Golgi ion homeostasis and vesicular Golgi trafficking (18). While TMEM165 has been extensively characterized in association with congenital disorders of glycosylation, its relationship with cancer remains to be determined. HCC-related proteins have been identified in multiple cellular compartments, including the nucleus, cytoplasm, mitochondria and plasma membrane. However, association of Golgi proteins with HCC has rarely been documented in the literature to date. To the best of our knowledge, GP73 (a 73-kDa Golgi transmembrane protein) is the protein that has been relatively well documented as a useful serum biomarker for HCC and shown to be involved in the progression of benign liver disease (17,19,20). In the present study, we identified a Golgi transmembrane protein, *TMEM165*, that is overexpressed in HCC patient tissues. *TMEM165* expression was significantly associated with high levels of α-fetoprotein as well as presence of macroscopic vascular and serosal invasion. Consistently, *TMEM165* depletion attenuated invasion activities of HCC cells via decrease in MMP-2 expression. Our findings revealed that *TMEM165* could serve as a novel HCC marker associated with cancer aggressiveness and presents a potential therapeutic target.

Materials and methods

Patients and tissue samples. HCC tissues were acquired from patients with HCC subjected to hepatic surgery between September 1992 and December 2004 at Korea Cancer Center Hospital. A total of 88 HCCs used in the present study included 33 pair-matched HCC and adjacent liver tissues, and 55 HCC tissues. Normal liver tissues were obtained from patients with colon or rectal cancer, metastasized into liver, who underwent surgical resection at Seoul National University Hospital and Korea Cancer Center Hospital. The adjacent liver tissues around these metastatic cancers were regarded and used as a normal liver (n=15) when liver fibrosis as well as HCC were not observed in the patients. Our study was approved by the Institutional Review Boards of Korea Cancer Center Hospital and Seoul National University Hospital. Written informed consent was either waived by the Institutional Review Board of Korea Cancer Center Hospital or received from patients at Seoul National University Hospital, respectively. Clinicopathological information collected retrospectively was utilized to examine associations between *TMEM165* expression patterns and HCC characteristics. Fibrosis was graded on a scale of 0-4 (stage 0, not present; stage 1, portal; stage 2, periportal; stage 3, septal; and stage 4, cirrhosis).

Cell culture and siRNA transfection. Cell lines were obtained from two institutions. The cell lines, SNU354, SNU398, SNU449, SNU475, SNU739 and Huh7 were purchased from the Korean Cell Line Bank (Seoul, South Korea) and the cell lines, Hep3B, HepG2, BJ, IMR90, WI38, normal Small Airway (PCS-301-010) and Prostate (PCS-440-010) epithelial cells from the American Type Culture Collection (ATCC; Manassas, VA, USA). Huh7, SNU354, SNU398, SNU449, SNU475 and SNU739 cells were cultured in RPMI-1640 medium (LM 011-01; Welgene, Daegu, Korea) and BJ, IMR90, WI38, HepG2 and Hep3B were cultured in MEM (LM 007-07; Welgene) supplemented with 10% (w/v) fetal bovine serum (FBS; JR Scientific, Inc., Woodland, CA, USA) and 1% (w/v) penicillin/streptomycin (Welgene) at 37°C. Normal small Airway and Prostate epithelial cells were cultured in Airway Epithelial Basal media (ATCC PCS 300-030) supplemented with Bronchial Epithelial Cell Growth kit (ATCC PCS-300-040) and Prostate Epithelial Cell Basal Medium (ATCC PCS-440-030) supplemented with Prostate Epithelial Cell Growth kit (ATCC PCS-440-040), respectively. For knockdown of *TMEM165*, siRNA transfection was performed using Lipofectamine RNA iMAX reagent (cat. no. 13778030; Invitrogen; Thermo Fisher Scientific, Inc., Waltham, MA, USA) according to the manufacturer's instructions. The following siRNA sequences were used: *TMEM165* siRNA#1, 5'-AGCCAUCAUGGCAAUGCGCUAUU-3' (sense) and 5'-UAGCGCAUUGCCAUGAUGGCUUU-3' (antisense); and *TMEM165* siRNA#2, 5'-UUGGGUAGGACACCCAAUAUA UU-3' (sense) and 5'-UAUAUUGGGUGUCCUACCCAA UU-3' (antisense).

RNA extraction and cDNA synthesis. Total RNA was extracted from cultured cells and fresh tissues using the RNeasy Mini Kit (cat. no. 74106; Qiagen, Inc., Valencia, CA, USA) according to the manufacturer's protocol. The quality and concentration of isolated total RNA were determined using a NanoDrop ND-1000 spectrophotometer (NanoDrop; Thermo Fisher Scientific, Inc., Wilmington, DE, USA). RNA samples were stored at -80°C until gene expression analysis. cDNA was synthesized using the iScript reverse transcriptase kit (cat. no. 170890; Bio-Rad Laboratories, Inc., Hercules, CA, USA) in keeping with the manufacturer's protocol.

Quantitative and semi-quantitative RT-PCR. Quantitative RT-PCR was performed with the KAPA SYBR FAST Universal qPCR kit (kit code: KK4301; Kapa Biosystems, Inc., Boston, MA, USA) on the CFX96 Real-Time RT-PCR Detection System (Bio-Rad Laboratories, Inc.). The primer sequences used for real-time RT-PCR were: *TMEM165* forward, 5'-GGCAGTAATTGGAGGAAGAATGATAGC-3' and reverse, 5'-ACCAGAATCAGGGCTTATAAATAGT GC-3'; and β2-microglobulin forward, 5'-AAGGACTGGTCT TTCTATCTCTTGTA-3' and reverse, 5'-ACTATCTTGG GGTGTGACAAAGTC-3'. Median Ct values from triplicate experiments were used for statistical analyses and *TMEM165* levels were normalized to median β2-microglobulin expression. Relative *TMEM165* expression in HCC and adjacent liver tissues, compared to that in normal liver tissues, was analyzed using the comparative threshold cycle $2^{-\Delta\Delta Ct}$ method. Semi-quantitative RT-PCR was performed using

the Maxime PCR PreMix kit (cat. no. 25185; iNtRON Biotechnology, Kyungi-do, Korea) and the following primers: *TMEM165* forward, 5'-GGCAGTAATTGGAGG AAGAATGATAGC-3' and reverse, 5'-ACCAGAATCAGG GCTTATAAATAGTGC-3'; β2-microglobulin forward, 5'-GTGCTCGCGCTACTCTCTCT-3' and reverse, 5'-CGG CAGGCATACTCATCTTT-3'; MMP-1 forward, 5'-ACA AAGTTGATGCAGTTTTCA-3' and reverse, 5'-GAATCC ATAAGCCACAAACTT-3'; MMP-2 forward, 5'-ATCTTT GCTGGAGACAAATTC-3' and reverse, 5'-AACTTCACG CTCTTCAGACTT-3'; MMP-9 forward, 5'-AACTTTGAC AGCGACAAGAA-3' and reverse, 5'-TTGAACAAATAC AGCTGGTTC-3'; MMP-13 forward, 5'-CCCAAAATTTTC TACCTCTGA-3' and reverse, 5'-TTTTGATGATGATGA AACCTG-3'; β-actin forward, 5'-GGACTTCGAGCAAGA GATGG-3' and reverse, 5'-AGCACTGTGTTGGCGTAC AG-3'; RPS26 forward, 5'-CCAAGGACAAGGCCATTA AG-3' and reverse, 5'-AGCACCCGCAGGTCTAAATC-3'; and GAPDH forward, 5'-GTCAGTGGTGGACCTGAC CT-3' and reverse, 5'-TGCTGTAGCCAAATTCGTTG-3'. The optimal PCR cycle for each primer set was determined by monitoring PCR products harvested at 2-cycle intervals with at least 3 different cycles. PCR amplification was performed with an initial 2 min of denaturation at 94°C, followed by cycling a 20 sec denaturation at 94°C, 10 sec annealing at 55°C and 30 sec extension at 72°C with a final 5 min extension at 72°C. The final PCR products were loaded on agarose gels and mRNA levels quantitated using NIH ImageJ software (http://rsb.info.nih.gov/ij).

Western blot analysis. Total tissue samples were homogenized in lysis buffer [50 mM Tris-HCl, pH 7.4, 150 mM NaCl, 5 mM EDTA, 1% (v/v) Nonidet P-40, 0.1% (w/v) sodium dodecyl sulfate, 0.5% (w/v) sodium deoxycholate] including protease inhibitor cocktail (cat. no. P3100-010; GenDEPOT, Inc., Barker, TX, USA) and placed on ice for 20 min. After incubation, tissues were centrifuged for 20 min at 13,000 x g at 4°C and the supernatant fractions were collected. Quantified and sampled proteins were separated on a 12.0% (w/v) SDS gel and transferred to nitrocellulose membranes (cat. no. 10401396; Whatman, Maidstone, UK). Next, the membranes were blocked with 5% (w/v) skim milk in TBS with Tween-20 (TBS-T) buffer [25 mM Tris-HCl, pH 7.4, 140 mM NaCl, 2.7 mM KCl, 0.05% (w/v) Tween-20] for 1 h at room temperature, followed by incubation with primary antibodies against TMEM165 (diluted to 1:1,000; cat. no. 20485-1-AP; ProteinTech Group, Rosemont, IL, USA) and GAPDH (diluted to 1:2,000; cat. no. sc-25778; Santa Cruz Biotechnology, Inc., Santa Cruz, CA, USA) for 1 h at room temperature. After washing 3 times with TBS-T, the membranes were treated with horseradish peroxidase-conjugated secondary antibody (diluted to 1:3,000; cat. nos. A120-101P and A90-116P; Bethyl Laboratories, Inc., Montgomery, TX, USA) at room temperature for 1 h. Following 3 further washes with TBS-T, the membranes were reacted with Luminol chemiluminescent reagent (cat. no. sc-2048; Santa Cruz Biotechnology, Inc.) according to the manufacturer's protocol. The intensities of the band were analyzed using the NIH ImageJ software (National Institutes of Health, Bethesda, MD, USA).

Figure 1. *TMEM165* is overexpressed in HCC. (A) *TMEM165* mRNA was visualized via semi-quantitative RT-PCR in 10 pair-matched HCC (T) and adjacent liver tissues (N). (B) Real-time RT-PCR results revealing relative mRNA levels of *TMEM165* quantitated in normal (n=15), adjacent liver (n=33), and HCC tissues (n=88). The sample set analyzed included 33 pair-matched tissues as indicated in Materials and methods. P-values were calculated by ANOVA Tukey's post hoc test. The horizontal line in the box plot is the median value, and the symbols, open circle (°) and asterisk (*) on the bars indicate outlier and extreme outlier samples, respectively, with 95% confidence interval. (C) Protein expression of TMEM165 in 7 pair-matched HCC and adjacent liver tissues determined using western blotting. β2-Microglobulin (β2M) and GAPDH were used as internal controls. The tissues used for A and C were randomly selected from the 33 pair-matched set. All semi-quantitative RT-PCR and western blotting experiments were repeated at least 3 times. The densitometry analysis was performed using ImageJ software. P-values were calculated by a two-sample t-test. *TMEM165*, transmembrane protein 165; HCC, human hepatocellular carcinoma.

Table I. Patient demographics and pathological data (n=88).

Variables	Classification	Distribution
Sex	Male : Female	77 : 11
Age (years)	Year, mean ± SD (range)	52.05±10.79 (25-74)
Etiology	Hepatitis B : Hepatitis C	85 : 03
Total bilirubin	<1 mg/dl : ≥1 mg/dl	59 : 29
AFP	<20 ng/dl : ≥20 ng/dl	38 : 49
	<50 ng/dl : ≥50 ng/dl	47 : 40
	<200 ng/dl : ≥200 ng/dl	55 : 32
AST	IU/l, mean ± SD (range)	51.92±31.07 (15-182)
ALT	IU/l, mean ± SD (range)	46.25±25.21 (10-130)
Child-Pugh classification	A : B and C	70 : 07
Tumor size	cm, mean ± SD (range)	5.8±3.25 (1.0-24.0)
Tumor number	Single : Multiple	59 : 17
Macroscopic vascular invasion	No : Yes	78 : 5
Microscopic vascular invasion	No : Yes	34 : 39
Serosal invasion	No : Yes	68 : 12
Edmondson grade[a]	I : II : III : VI	11 : 48 : 27 : 1
Fibrosis	0 : 1 : 2 : 3 : 4	3 : 7 : 16 : 24 : 29

[a]Edmondson-Steiner histological grade. In our present patient cohort, the clinicopathological information collected retrospectively has missing data, since some parameters were not obtained from all patients. AFP, α-fetoprotein; AST, aspartate aminotransferase; ALT, alanine transaminase.

Clonal survival analysis. Huh7 and SNU475 cells were transiently transfected with control and *TMEM165* siRNAs. At 24 h after transfection, 1,000 cells were seeded on a 6-well plate. Cells were fixed with 10% (w/v) formaldehyde and stained with 0.1% (w/v) crystal violet 10 days after seeding. Colonies were counted using digital images obtained with ImageJ. All experiments were performed in triplicate.

Invasion analysis. Polycarbonate membrane Transwell inserts (cat. no. 354480; Corning Inc., Corning, NY, USA) were coated with 20 µg/ml Matrigel. Following transient transfection, Huh7 and SNU475 cells (2x10⁴) were seeded on the upper compartment of the chamber in serum-free medium. As a chemoattractant, complete medium containing 10% (v/v) FBS was placed in the bottom compartment. After 24 and 48 h of incubation, the cells were fixed, stained with Hemacolor® solution (Merck KGaA, Darmstadt, Germany) and counted under a light microscope in 4 different fields. All experiments were performed in triplicate.

Statistical analysis. Statistical analysis was performed using SPSS v.23.0 software (IBM Corp., Armonk, NY, USA). Receiver operating characteristic (ROC) curves were generated to assess the optimal cut-off point for *TMEM165* expression. A one-way analysis of variance (ANOVA) with post hoc Tukey's HSD test was conducted to compare the expression levels of *TMEM165* in normal, non-tumor and tumor samples. Correlations between *TMEM165* expression and clinicopathological parameters were determined using a 2-sample t-test, Pearson's correlation test, Chi-squared (χ^2) and Fisher's exact tests. For the comparison of invasion and clonal survival, ANOVA with post hoc Dunnett's test was performed. The data were considered significant at P<0.05.

Results

TMEM165 is overexpressed in HCC. To establish whether TMEM165 is involved in the pathogenesis of HCC, we examined its expression patterns in tumor and adjacent liver tissue specimens obtained from HCC patients subjected to surgical resection. Semi-quantitative RT-PCR disclosed higher *TMEM165* expression in HCC than adjacent liver tissues (P=0.027) (Fig. 1A). To confirm *TMEM165* expression, we performed quantitative real-time RT-PCR on an extended HCC sample set (n=88) (Table I) comprised of background liver cirrhosis (n=29) and fibrosis (n=3:7:16:24:29 for grades 0:1:2:3:4, respectively). Similar to semi-quantitative RT-PCR findings, real-time RT-PCR revealed significantly elevated *TMEM165* expression in HCC, compared to adjacent non-tumor liver (P<0.001) and normal liver tissues (P=0.034) (Fig. 1B). In contrast to tumor tissues, adjacent liver tissues did not exhibit a significant difference in *TMEM165* expression, compared to normal liver tissues (P=0.942). When expression levels were adjusted and compared with those of normal liver tissues, the mean increases in *TMEM165* expression in HCC and adjacent liver tissues were 2.40- and 1.02-fold (median, 1.89- and 0.99-fold, respectively). Consistent with the mRNA expression data, the protein levels were higher in HCC than adjacent liver tissues (P=0.002) (Fig. 1C). The collective findings clearly demonstrated *TMEM165* overexpression in HCC.

TMEM165 overexpression is clinically associated with macroscopic vascular invasion, microscopic serosal invasion, and high α-fetoprotein levels of HCC. Next, we examined the potential association of *TMEM165* mRNA levels with clinico-pathological parameters to ascertain whether overexpression has a clinical impact on HCC. Variations in *TMEM165* expression determined based on real-time analysis were mostly <2.0-fold between normal and adjacent liver tissues. To further verify an optimal cut-off point for *TMEM165* expression, we performed ROC analysis using SPSS software. In the analysis, the clinical parameters, AFP level (<50 vs. ≥50 ng/ml), macroscopic invasion (no and yes) and serosal invasion (no and yes) were associated with *TMEM165* (P<0.05). The optimal cut-off points of *TMEM165* expression for these parameters were 1.98- (P=0.009), 3.03- (P=0.032), and 2.32-fold (P=0.018), respectively, indicating a 2.0-fold is suitable for comparison with clinicopathological parameters. Accordingly, we subdivided HCCs into two groups based on *TMEM165* expression employing 2.0-fold as a cut-off point. Among the 88 tumor tissues examined, 41 (46.6%) exhibited ≥2.0-fold increase in *TMEM165* transcript expression. Consistent with the ROC analysis, higher α-fetoprotein levels (≥50 ng/ml, P=0.022; ≥200 ng/ml, P=0.024) and presence of macroscopic vascular invasion (P=0.023) and serosal invasion (P=0.006) were significantly associated with *TMEM165* overexpression (≥2.0-fold) (Table II). In contrast, HCC-based parameters such as sex (P=0.187), age (P=0.479), aspatate transaminase (P=0.204), alanine transaminase (P=0.386), Child-Pugh classification (P=0.273), tumor size (P=0.113), tumor number (P=0.212), microscopic vascular invasion (P=0.377), Edmondson grade (P=0.274) and cirrhosis (P=0.334), were not associated with *TMEM165* overexpression. Furthermore, HCCs classified based on significant parameters (Table II) exhibited marked differences in *TMEM165* expression (Fig. 2). Specifically, the *TMEM165* expression level was positively correlated with the AFP level (Fig. 2A) (n=87, r=0.213 and P=0.048). Additionally, median increases in *TMEM165* expression were 1.90- and 3.26-fold according to macroscopic vascular invasion (no and yes, P=0.034) (Fig. 2B) and 1.87- and 2.95-fold according to serosal invasion (no and yes, P=0.03), respectively (Fig. 2C). The clinicopathological association data indicated that *TMEM165*-associated parameters influence aggressiveness of HCCs, based on the finding that overexpression of this protein is clinically associated with the invasive characteristics of this tumor type.

TMEM165 depletion decreases invasion of HCC cells without affecting clonal survival. In view of the clinical association of *TMEM165* overexpression with macroscopic vascular and serosal invasion, we further investigated the possibility of regulatory effects on the invasion of HCC cells. Prior to evaluation, we determined the expression patterns of *TMEM165* in normal and cancer cell lines to select suitable cells. For this experiment, we employed the established HCC cell lines Hep3B, Huh7, SNU354, SNU398, SNU449, SNU475 and SNU739 and hepatoblastoma cell line HepG2. Consistent with data from HCC specimens, most cancer cell lines exhibited greater expression than normal human fibroblast (BJ, Wi38, IMR90) and epithelial cells, including those of the Small Airway and Prostate (Fig. 3A).

Table II. Correlation between TMEM165 expression and clinicopathological parameters (n=88).

Variables	TMEM165 expression		P-value[a]
	<2.0 fold	≥2.0 fold	
Sex			
Male	43	34	0.187
Female	4	7	
Age (years)			
<52	20	19	0.479
≥52	26	22	
AFP (ng/ml)			0.149
<20	23	15	
≥20	23	26	
AFP (ng/ml)			**0.022**
<50	30	17	
≥50	16	24	
AFP (ng/ml)			**0.024**
<200	34	21	
≥200	12	20	
AST (U/l)			
<40	20	22	0.204
≥40	27	19	
ALT (U/l)			
<35	17	17	0.386
≥35	30	24	
Child-Pugh classification			
A	36	34	0.273
B,C	5	2	
Tumor size (cm)			
<5	26	16	0.113
≥5	21	24	
Tumor number			
Single	33	26	0.212
Multiple	7	10	
Macroscopic vascular invasion			
No	43	35	**0.023**
Yes	0	5	
Microscopic vascular invasion			
No	17	17	0.377
Yes	22	17	
Serosal invasion			
No	41	27	**0.006**
Yes	2	10	
Edmondson grade			
I,II	33	26	0.274
III,IV	13	15	
Cirrhosis			
No	28	22	0.334
Yes	14	15	

[a]Significance of *TMEM165* overexpression in association with clinicopathological parameters was calculated using the Chi-Square test; [b]Bold indicates P<0.05. AFP, α-fetoprotein; AST, aspartate aminotransferase; ALT, alanine transaminase.
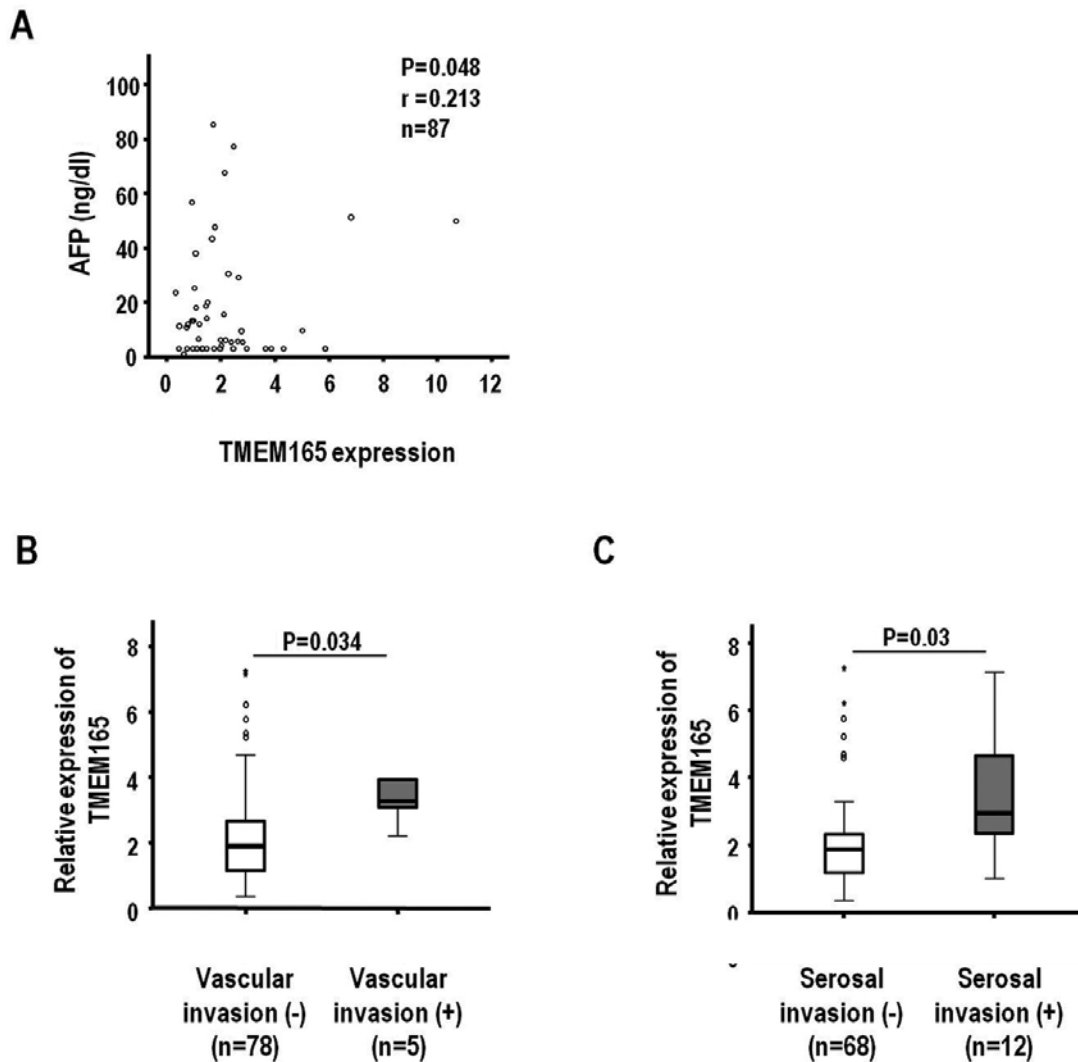
Figure 2. *TMEM165* expression in HCC is correlated with aggressive clinical parameters. (A) The correlation between the levels of *TMEM165* and AFP was analyzed using Pearson's correlation test. (B and C) HCC samples were classified into two subgroups based on significant clinicopathological parameters (Table II), including (B) macroscopic vascular invasion and (C) serosal invasion. Using real-time RT-PCR results from Fig. 1B, differences in *TMEM165* mRNA levels between the subgroups were analyzed by a two-sample t-test. Open circle (°) and asterisk (*) are the outlier and extreme outlier samples, respectively, with 95% confidence interval and the horizontal line indicates median value. *TMEM165*, transmembrane protein 165; HCC, human hepatocellular carcinoma; AFP, α-fetoprotein.

Next, we examined the effect of *TMEM165* depletion on invasion of Huh7 cells that express high levels of *TMEM165*. Notably, *TMEM165* depletion achieved via transfection of siRNA induced a significant decrease in the invasive activity of Huh7 cells (Fig. 3B). Two siRNAs (#1 and #2) recognizing different regions on the coding sequence induced a noticeable level of suppression of invasive activity (51.3 and 72.1%, respectively, compared to the control siRNA). Significantly reduced invasion was additionally observed in the SNU475 cell line (Fig. 3C). The rates of inhibition of invasion by *TMEM165* siRNA #1 and #2 were 88.2 and 95.7%, respectively, clearly indicating that knockdown of *TMEM165* in HCC suppresses invasive activity to a significant extent. To further confirm this finding, we assessed the effects of *TMEM165* depletion on clonal growth that can detect cell proliferation and death. Notably, clonal growth was hardly inhibited in both cell lines after transfection of *TMEM165* siRNAs (P>0.1, Fig. 4A and B). Thus, the *TMEM165* depletion-mediated suppression of HCC

cell invasion activity was not attributable to decreased clonal survival.

TMEM165 affects matrix metalloproteinase-2 (MMP-2) expression. To further determine the mechanisms underlying *TMEM165*-mediated regulation of invasion, we examined the potential involvement of MMPs, well-known invasion activators. Specifically, we assessed the expression levels of *MMP-1, -2* and *-9* in HCC cells depleted of *TMEM165*. As expected from the cell invasion data, *MMP-2* levels were severely decreased under conditions of *TMEM165* depletion in both Huh7 and SNU475 cell lines (Fig. 5A and B). In contrast, *MMP-1* and *-9* levels were not affected. To determine whether TMEM165 controls cancer cell invasion in a similar manner to Golgi phosphoprotein 2, we examined the expression of *MMP-13* that are regulated by Golgi phosphoprotein 2 (21). Notably, *TMEM165* depletion had no effect on the expression patterns of this molecule, indicating that the mechanism by
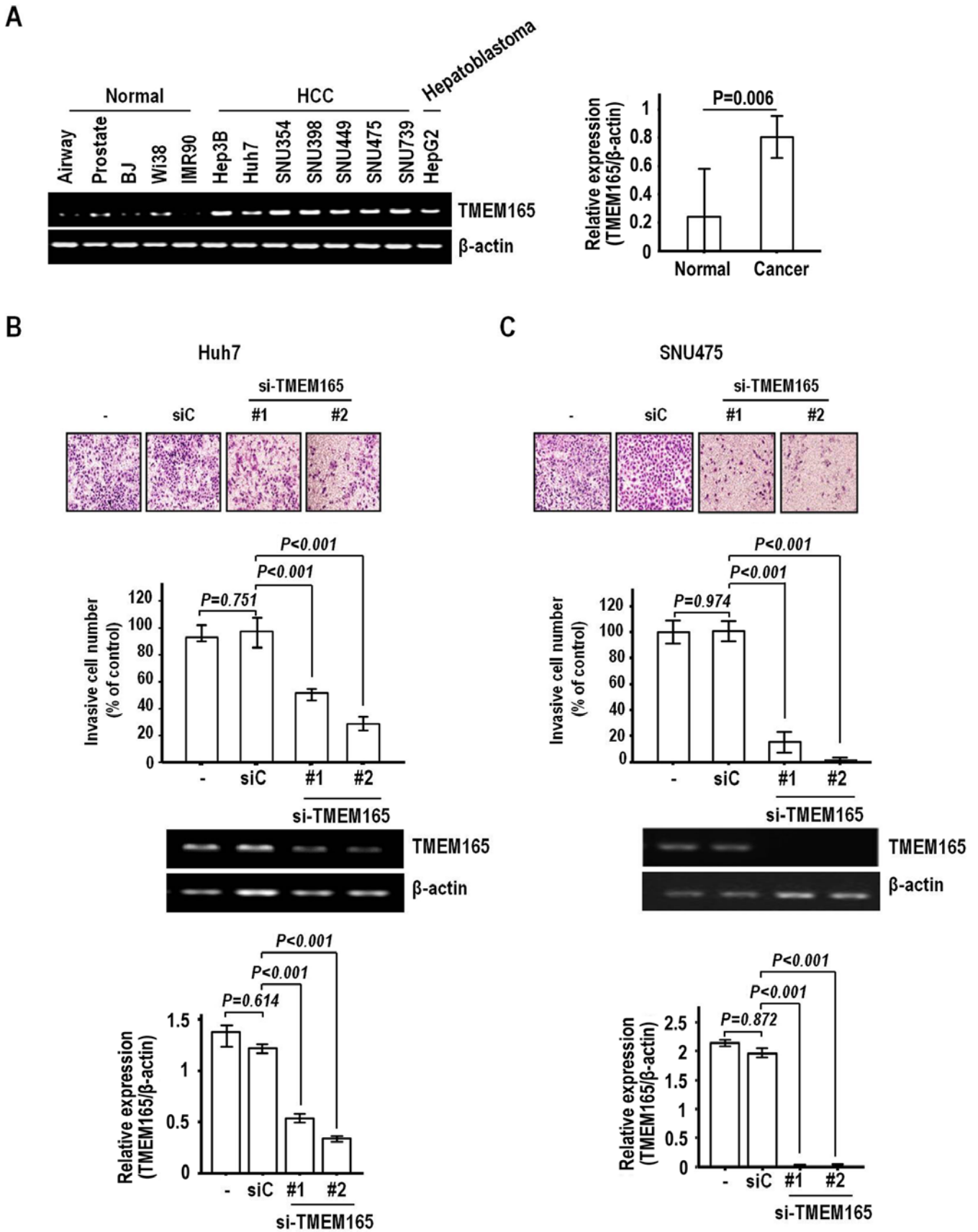
Figure 3. *TMEM165* depletion weakens the invasive activity of HCC cells. (A) *TMEM165* expression was assessed in normal human fibroblasts, epithelial cells and various HCC cell lines via semi-quantitative RT-PCR using β-actin as an internal control. (B and C) *TMEM165* siRNA (#1 and #2) or control-siRNA (siC)-transfected Huh7 (B) and SNU475 cells (C) were loaded onto a Matrigel-coated invasion chamber. Invading cells were stained with crystal violet and visualized under a microscope (magnification, x100). RT-PCR analysis of *TMEM165* depletion following siRNA transfection. Invasion rates were calculated by dividing the counts (invading cells) of *TMEM165*-transfected cells with those of control siRNA-transfected cells. The mean ± SD of calculated cells were plotted, with P-values calculated by ANOVA with Dunnett's test. The densitometry analysis was performed using ImageJ software. *TMEM165*, transmembrane protein 165; HCC, human hepatocellular carcinoma.

A

Huh7

B
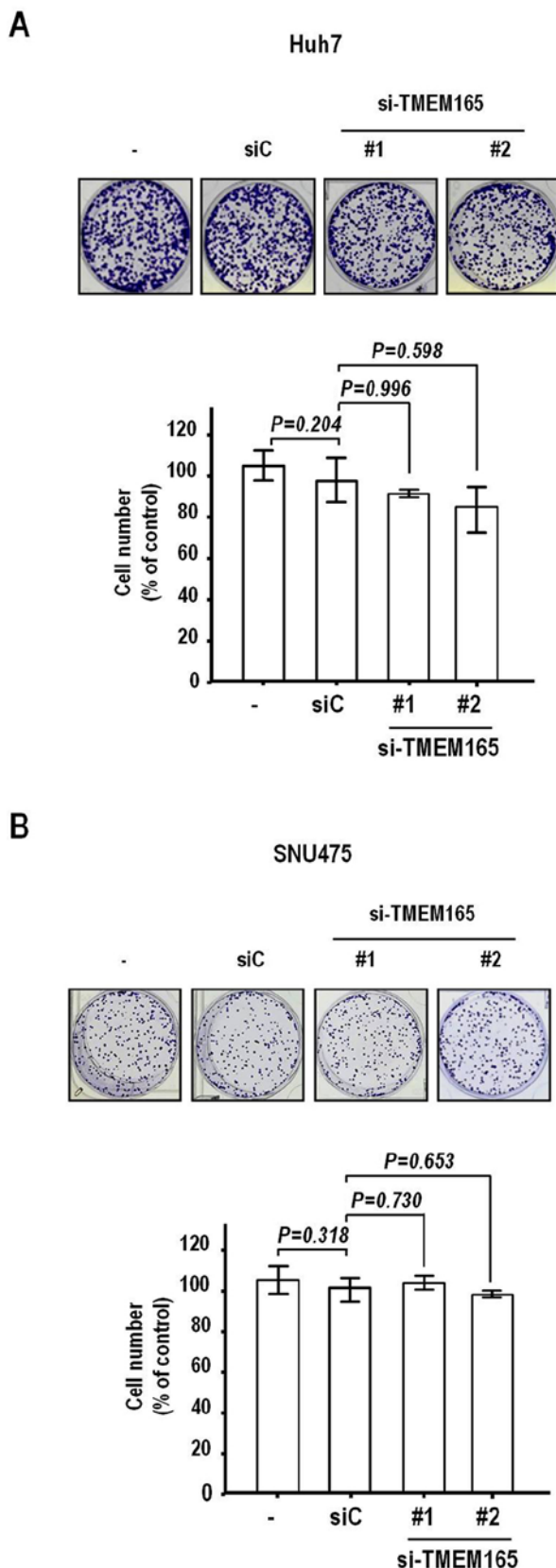
SNU475

Figure 4. *TMEM165* depletion has no impact on clonal survival of HCC cells. siRNA-transfected Huh7 (A) and SNU475 cells (B) were seeded at low density, and the surviving colonies were stained with crystal violet and visualized under a microscope (magnification, x100). Survival rates were calculated by dividing the counts (surviving cells) of *TMEM165*-siRNA (#1 and #2)-transfected cells with those of control siRNA (siC)-transfected cells. Bars represent the mean ± SD, with P-values calculated by ANOVA with Dunnett's test. *TMEM165*, transmembrane protein 165; HCC, human hepatocellular carcinoma.

A

Huh7

B
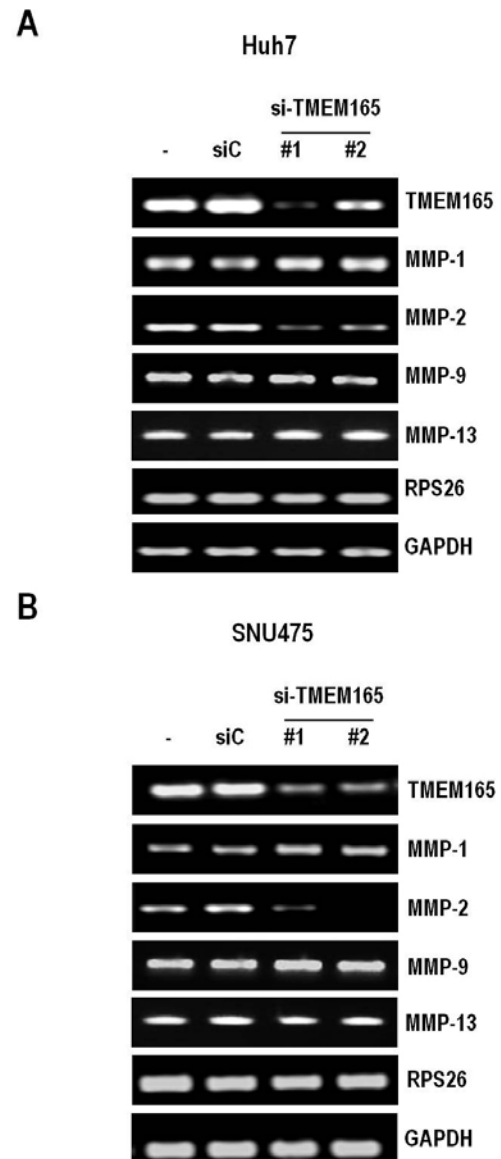
SNU475

Figure 5. TMEM165 controls MMP-2 expression. *TMEM165*-depleted Huh7 (A) and SNU475 cells (B) were prepared by transfection with targeted siRNAs and grown in 5% serum for 48 h. MMP-1, -2, -9 and -13 mRNA levels were assessed using RT-PCR. Ribosomal protein S26 (RPS26) and GAPDH were used as internal controls. *TMEM165*, transmembrane protein 165; MMP, matrix metalloproteinase.

which TMEM165 promotes the invasive activity of cancer cells is distinct from that of Golgi phosphoprotein 2.

Discussion

The TMEM165 protein, mainly characterized in association with congenital disorders of glycosylation type 2 disease, has recently attracted significant research attention (13,14,22,23). Based on cohort studies, 3 different mutations in *TMEM165* have been reported to date, specifically, homozygous point mutation in the deep intronic splice region, homozygous missense mutation and heterozygous missense mutation, all of which culminate in loss or decrease in function of the protein (11,14). Recent *in vitro* studies have disclosed that TMEM165 is associated with Golgi homeostasis sensitive to

manganese concentrations (18), indicating that mutation and loss of function of the protein can trigger defects in manganese-sensitive Golgi homeostasis. The importance of Golgi proteins in promoting cancer progression has been highlighted in previous studies. Golgi phosphoprotein 2 (GP73) is aberrantly expressed in HCC and knockdown of this gene inhibits cancer cell invasiveness via altering expression of E-cadherin, N-cadherin and MMP-13 (24,25). Moreover, Golgi phosphoprotein 3 (GOLPH3) is overexpressed in various cancer types, in turn, increasing invasion and migration of cancer cells (26-28). GOLPH3 interacts with phosphatidylinositol-4-phosphate and myosin18A to facilitate Golgi to plasma membrane trafficking and regulates the directional migration of cells (29). Despite the recent focus on Golgi proteins, the specific function of TMEM165 in cancer remains to be determined.

We previously established an integrative analysis tool to determine the gene expression patterns between non-tumor and tumor regions in correlation with clinical outcomes (6). Based on these experiments, we demonstrated for the first time that the TMEM165 protein is significantly upregulated in tumor compared to non-tumor tissues of HCC patients. Notably, overexpression of *TMEM165* (using the 2-fold cut-off criterion) was positively correlated with aggressiveness of HCC characterized by high AFP levels as well as presence of macroscopic vascular and microscopic serosal invasion. In keeping with this finding, depletion of *TMEM165* significantly reduced invasiveness of human HCC cell lines *in vitro*, accompanied by a decrease in expression of *MMP-2*, an endopeptidase that degrades the extracellular matrix to stimulate cancer invasion and metastasis. However, other *MMPs (MMP-1, -9,* and *-13)* were not affected by depletion of *TMEM165*. These results support a role of TMEM165 as a key molecule that directs cancer cell invasion, consequently promoting aggressiveness. Clonal survival analysis can be effectively used to detect several phenotypic changes, including proliferation, death and senescence. *TMEM165* depletion decreased cancer cell invasion without affecting clonal survival, indicative of a negligible effect on these phenotypes. Inhibition of cellular proliferation, death or senescence is reported to trigger a decrease in the invasion rate of cancer cells (30). Therefore, TMEM165 regulation of cancer cell invasion is credible, since the possibility that phenotypic changes, such as cellular proliferation, death, and senescence, can affect cancer cell invasion was eliminated.

Despite the significant correlation between *TMEM165* overexpression and aggressiveness of the tumor phenotype, *TMEM165* was not associated with patient prognosis in the current study (data not shown). This may be attributable to the small number of samples used for our analysis. Studies on larger cohorts are therefore required to validate the expression patterns of *TMEM165* in relation to patient prognosis. Furthermore, while decreased invasiveness of cancer cells upon *TMEM165* knockdown was evident, the precise mechanisms require elucidation in future studies. Considering the relationship between *TMEM165* mutation and type II congenital disorder of glycosylation, it is plausible that its overexpression in HCC is associated with abnormalities in galactosylation and sialylation of N-glycoproteins observed in the disease. These protein modifications influence the invasive activity of cancer cells (31). Several invasion-related proteins (CD44, integrin and E-cadherin) have been revealed to be markedly affected by glycosylation (32-34). In summary, *TMEM165* is both transcriptionally and translationally overexpressed in HCC and associated with invasive activity.

Availability of data and materials

The datasets used during the present study are available from the corresponding author upon reasonable request.

Authors' contributions

KHL, SBK and JH conceived and supervised the study. KHL, JSL and MYK wrote the manuscript. SBK and ERP reviewed and edited manuscript. MYK, JSL, ERP, YNS and JYJ prepared material and/or performed experiment. JSL and MYK performed statistical analysis. EHC, SHP, CJH, DWC, JJJ, KSS and SBK generated clinical data. All authors read and approved the manuscript and agree to be accountable for all aspects of the research in ensuring that the accuracy or integrity of any part of the work are appropriately investigated and resolved.

Ethics approval and consent to participate

The present study was approved by the Institutional Review Boards of Korea Cancer Center Hospital and Seoul National University Hospital. Written informed consent was either waived by the Institutional Review Board of Korea Cancer Center Hospital or received from patients at Seoul National University Hospital, respectively.

Patient consent for publication

Not applicable.

Competing interests

The authors declare that they have no competing interests.

References

1. Torre LA, Bray F, Siegel RL, Ferlay J, Lortet-Tieulent J and Jemal A: Global cancer statistics, 2012. CA Cancer J Clin 65: 87-108, 2015.
2. El-Serag HB: Hepatocellular carcinoma. N Engl J Med 365: 1118-1127, 2011.
3. Bruix J and Sherman M: American Association for the Study of Liver Diseases: Management of hepatocellular carcinoma: An update. Hepatology 53: 1020-1022, 2011.

 4. Llovet JM, Ricci S, Mazzaferro V, Hilgard P, Gane E, Blanc JF, de Oliveira AC, Santoro A, Raoul JL, Forner A, *et al*: Sorafenib in advanced hepatocellular carcinoma. N Engl J Med 359: 378-390, 2008.
 5. Cheng AL, Kang YK, Chen Z, Tsao CJ, Qin S, Kim JS, Luo R, Feng J, Ye S, Yang TS, *et al*: Efficacy and safety of sorafenib in patients in the Asia-Pacific region with advanced hepatocellular carcinoma: A phase III randomised, double-blind, placebo-controlled trial. Lancet Oncol 10: 25-34, 2009.
 6. Kim BY, Suh KS, Lee JG, Woo SR, Park IC, Park SH, Han CJ, Kim SB, Jeong SH, Yeom YI, *et al*: Integrated analysis of prognostic gene expression profiles from hepatitis B virus-positive hepatocellular carcinoma and adjacent liver tissue. Ann Surg Oncol 19 (Suppl 3): S328-S338, 2012.
 7. Kim BY, Choi DW, Woo SR, Park ER, Lee JG, Kim SH, Koo I, Park SH, Han CJ, Kim SB, *et al*: Recurrence-associated pathways in hepatitis B virus-positive hepatocellular carcinoma. BMC Genomics 16: 279, 2015.
 8. Park ER, Kim SB, Lee JS, Kim YH, Lee DH, Cho EH, Park SH, Han CJ, Kim BY, Choi DW, *et al*: The mitochondrial hinge protein, UQCRH, is a novel prognostic factor for hepatocellular carcinoma. Cancer Med 6: 749-760, 2017.
 9. Potelle S, Morelle W, Dulary E, Duvet S, Vicogne D, Spriet C, Krzewinski-Recchi MA, Morsomme P, Jaeken J, Matthijs G, *et al*: Glycosylation abnormalities in Gdt1p/TMEM165 deficient cells result from a defect in Golgi manganese homeostasis. Hum Mol Genet 25: 1489-1500, 2016.
10. Rosnoblet C, Legrand D, Demaegd D, Hacine-Gherbi H, de Bettignies G, Bammens R, Borrego C, Duvet S, Morsomme P, Matthijs G, *et al*: Impact of disease-causing mutations on TMEM165 subcellular localization, a recently identified protein involved in CDG-II. Hum Mol Genet 22: 2914-2928, 2013.
11. Foulquier F, Amyere M, Jaeken J, Zeevaert R, Schollen E, Race V, Bammens R, Morelle W, Rosnoblet C, Legrand D, *et al*: TMEM165 deficiency causes a congenital disorder of glycosylation. Am J Hum Genet 91: 15-26, 2012.
12. Bammens R, Mehta N, Race V, Foulquier F, Jaeken J, Tiemeyer M, Steet R, Matthijs G and Flanagan-Steet H: Abnormal cartilage development and altered N-glycosylation in Tmem165-deficient zebrafish mirrors the phenotypes associated with TMEM165-CDG. Glycobiology 25: 669-682, 2015.
13. Schulte Althoff S, Grüneberg M, Reunert J, Park JH, Rust S, Mühlhausen C, Wada Y, Santer R and Marquardt T: TMEM165 deficiency: Postnatal changes in Glycosylation. JIMD Rep 26: 21-29, 2016.
14. Dulary E, Potelle S, Legrand D and Foulquier F: TMEM165 deficiencies in Congenital Disorders of Glycosylation type II (CDG-II): Clues and evidences for roles of the protein in Golgi functions and ion homeostasis. Tissue Cell 49: 150-156, 2017.
15. Jaeken J, Schachter H, Carchon H, De Cock P, Coddeville B and Spik G: Carbohydrate deficient glycoprotein syndrome type II: A deficiency in Golgi localised N-acetyl-glucosaminyltransferase II. Arch Dis Child 71: 123-127, 1994.
16. Peters V, Penzien JM, Reiter G, Körner C, Hackler R, Assmann B, Fang J, Schaefer JR, Hoffmann GF and Heidemann PH: Congenital disorder of glycosylation IId (CDG-IId) - A new entity: Clinical presentation with Dandy-Walker malformation and myopathy. Neuropediatrics 33: 27-32, 2002.
17. Martinez-Duncker I, Dupré T, Piller V, Piller F, Candelier JJ, Trichet C, Tchernia G, Oriol R and Mollicone R: Genetic complementation reveals a novel human congenital disorder of glycosylation of type II, due to inactivation of the Golgi CMP-sialic acid transporter. Blood 105: 2671-2676, 2005.
18. Potelle S, Dulary E, Climer L, Duvet S, Morelle W, Vicogne D, Lebredonchel E, Houdou M, Spriet C, Krzewinski-Recchi MA, *et al*: Manganese-induced turnover of TMEM165. Biochem J 474: 1481-1493, 2017.
19. Marrero JA, Romano PR, Nikolaeva O, Steel L, Mehta A, Fimmel CJ, Comunale MA, D'Amelio A, Lok AS and Block TM: GP73, a resident Golgi glycoprotein, is a novel serum marker for hepatocellular carcinoma. J Hepatol 43: 1007-1012, 2005.
20. Wei H, Li B, Zhang R, Hao X, Huang Y, Qiao Y, Hou J, Li X and Li X: Serum GP73, a marker for evaluating progression in patients with chronic HBV infections. PLoS One 8: e53862, 2013.
21. Jin D, Tao J, Li D, Wang Y, Li L, Hu Z, Zhou Z, Chang X, Qu C and Zhang H: Golgi protein 73 activation of MMP-13 promotes hepatocellular carcinoma cell invasion. Oncotarget 6: 33523-33533, 2015.
22. Krzewinski-Recchi MA, Potelle S, Mir AM, Vicogne D, Dulary E, Duvet S, Morelle W, de Bettignies G and Foulquier F: Evidence for splice transcript variants of *TMEM165*, a gene involved in CDG. Biochim Biophys Acta 1861: 737-748, 2017.
23. Morelle W, Potelle S, Witters P, Wong S, Climer L, Lupashin V, Matthijs G, Gadomski T, Jaeken J, Cassiman D, *et al*: Galactose supplementation in patients with TMEM165-CDG rescues the glycosylation defects. J Clin Endocrinol Metab 102: 1375-1386, 2017.
24. Chen X, Wang Y, Tao J, Shi Y, Gai X, Huang F, Ma Q, Zhou Z, Chen H, Zhang H, *et al*: mTORC1 up-regulates GP73 to promote proliferation and migration of hepatocellular carcinoma cells and growth of xenograft tumors in mice. Gastroenterology 149: 741-752, 2015.
25. Yang Y, Liu Q, Zhang H, Zhao H, Mao R, Li Z, Ya S, Jia C and Bao Y: Silencing of GP73 inhibits invasion and metastasis via suppression of epithelial-mesenchymal transition in hepatocellular carcinoma. Oncol Rep 37: 1182-1188, 2017.
26. Ma Y, Wang X, Wu Y, Sun B, Lv H, Rong F and Zheng X: Overexpression of GOLPH3 protein is associated with worse prognosis in patients with epithelial ovarian cancer. Tumour Biol 35: 11845-11849, 2014.
27. Li Q, Ma Y and Xu W: High GOLPH3 expression is associated with poor prognosis and invasion of hepatocellular carcinoma. Mol Med Rep 11: 4315-4320, 2015.
28. Li W, Guo F, Gu M, Wang G, He X, Zhou J, Peng Y, Wang Z and Wang X: Increased expression of GOLPH3 is associated with the proliferation of prostate cancer. J Cancer 6: 420-429, 2015.
29. Taft MH, Behrmann E, Munske-Weidemann LC, Thiel C, Raunser S and Manstein DJ: Functional characterization of human myosin-18A and its interaction with F-actin and GOLPH3. J Biol Chem 288: 30029-30041, 2013.
30. Schaeffer D, Somarelli JA, Hanna G, Palmer GM and Garcia-Blanco MA: Cellular migration and invasion uncoupled: Increased migration is not an inexorable consequence of epithelial-to-mesenchymal transition. Mol Cell Biol 34: 3486-3499, 2014.
31. Pinho SS and Reis CA: Glycosylation in cancer: Mechanisms and clinical implications. Nat Rev Cancer 15: 540-555, 2015.
32. English NM, Lesley JF and Hyman R: Site-specific de-N-glycosylation of CD44 can activate hyaluronan binding, and CD44 activation states show distinct threshold densities for hyaluronan binding. Cancer Res 58: 3736-3742, 1998.
33. Guo HB, Lee I, Kamar M, Akiyama SK and Pierce M: Aberrant N-glycosylation of beta1 integrin causes reduced alpha5beta1 integrin clustering and stimulates cell migration. Cancer Res 62: 6837-6845, 2002.
34. Pinho SS, Seruca R, Gärtner F, Yamaguchi Y, Gu J, Taniguchi N and Reis CA: Modulation of E-cadherin function and dysfunction by N-glycosylation. Cell Mol Life Sci 68: 1011-1020, 2011.